Sustainable Development Research; Vol. 3, No. 3; 2021
ISSN 2690-9898 E-ISSN 2690-9901
https://doi.org/10.30560/sdr.v3n3p17

Hydrolytic Degradation of 3D-Printed Poly (Lactic Acid) Structures

Logan Mulderrig[1,2], Franchino Chambers[1,2,3], Taylor A. Isais[4], Richard Jeske[1], Yan Li[1], Justin Kennemur[4] & Daniel Hallinan Jr.[1,2]

[1] Department of Chemical and Biomedical Engineering, Florida A&M University-Florida State University College of Engineering, Tallahassee, FL, USA

[2] Aero-propulsion, Mechatronics, and Energy Center, FAMU-FSU College of Engineering, Tallahassee, FL, US

[3] Department of Mechanical Engineering, Howard University, Washington, DC, USA

[4] Department of Chemistry & Biochemistry, Tallahassee, FL, USA

Correspondence: Daniel Hallinan Jr., Chemical and Biomedical Engineering, 2525 Pottsdamer Street, Suite A131, Tallahassee, FL 32310, USA. Tel: 1-850-645-0131. E-mail: dhallinan@eng.famu.fsu.edu

Received: September 17, 2021 Accepted: October 20, 2021 Online Published: October 28, 2021

The research was financed by the FAMU CREST Center (NSF award number 1735968), and REU support was provided by NSF award numbers 1560337 and 1646897.

Abstract

Hydrolytic degradation of commercially available 3D printing filament, i.e. poly (lactic acid) with broad molecular weight distribution was induced by incubating 3D-printed parts in deionized water at 3 temperatures. Small changes in orthogonal dimensions occurred due to relaxation of printing stresses, but no mass or volume loss were detected over the time-frame of the experiments. Molecular weight decreased while polydispersity remained constant. The most sensitive measure of degradation was found to be nondestructive, small-amplitude oscillatory tensile measurements. A rapid decay of tensile storage modulus was found with an exponential decay time constant of about an hour. This work demonstrates that practical monitoring of commercially available PLA degradation can be achieve with linear viscoelastic measurements of modulus.

Keywords: PLA properties, Hydrolysis, Chain scission, Modeling, 3D printing, modulus

1. Introduction

3D printing is a relatively new form of manufacturing that has been widely adopted since the expiration of the patent for fused deposition modeling (FDM) in 2009.(Crump, 1992) It has revolutionized the design, construction, and availability of custom parts in sectors including medical, aeronautical, automotive, military, and personal.(Ali Md, Batai, & Sarbassov, 2019) This is primarily due to competition driving down prices and the capability to rapidly prototype parts with FDM.(Ali Md et al., 2019) As 3D printing becomes more ubiquitous, the limitations and potential pitfalls must undergo further investigations. Specifically, structural integrity and sustainability are important to address, especially for FDM prepared parts. (Yao, Deng, Zhang, & Li, 2019)

The recognition of the impact of plastic waste on the health of the planet, as well as the finite quantity of fossil fuels has motivated research into more sustainable plastics. A plastic that has been used extensively in 3D printing is poly(lactic acid) (PLA). PLA is a naturally derived aliphatic polyester which is biocompatible and biodegradable.(Farah, Anderson, & Langer, 2016) It is also inexpensive and commercially produced by condensation polymerization of lactic acid, that is derived from fermentation of corn, sugar cane, and tapioca plants.(Jamshidian, Tehrany, Imran, Jacquot, & Desobry, 2010) The polycondensation reaction produces low molecular weight PLA pre-polymer, that is further driven to high molar mass through solid-state annealing. Alternatively, the cyclic dimer of lactic acid, known as lactide, can undergo ring-opening polymerization (ROP) to form high molar mass PLA.(Masutani & Kimura, 2018; Mehta, Kumar, Bhunia, & Upadhyay, 2005) The biodegradability of PLA can be attributed to ester linkages within the backbone that are susceptible to hydrolytic cleavage. Yet another advantage of PLA over fossil-fuel-derived polymers is lower carbon dioxide emissions over its lifecycle.(Vink, Rábago, Glassner, & Gruber, 2003) It can even serve as a carbon sink if it is produced with renewable energy.(Jamshidian et al., 2010; Vink & Davies, 2015) PLA has superior modulus to rigid polyolefin polymers, but poorer toughness.(Dorgan, Lehermeier, & Mang, 2000) It melts at a much lower temperature than

traditional high-performance polymers such as polyether ether ketone (PEEK) allowing for inexpensive processing and industrial composting.(Jamshidian et al., 2010)

Coupled with its degradability, PLA has found wide-spread adoption as a more sustainable alternative to polyolefins in food packaging and for agricultural mulching.(Masutani & Kimura, 2018) From the structural polymer perspective, the susceptibility of PLA to hydrolysis, especially at high temperatures, can lead to failure in applications with harsh environments.(Agrawal, Huang, Schmitz, & Athanasiou, 1997; Weir, Buchanan, Orr, Farrar, & Dickson, 2004) One such environment where this can be beneficial or problematic is in biomedical devices. The primary benefit is that it is bioabsorbable.(Masutani & Kimura, 2018) The problem is that hydrolysis of the polymer backbone can dramatically change the physical properties of the device and cause complications if degradation occurs more rapidly than desired. The primary degradation product of PLA is lactic acid, which can further degrade into carbon dioxide and water and be easily excreted through the kidneys or exhaled.[9] Biomedical applications of PLA consist of screws, plates, drug delivery, grafts, cavity filling, bone scaffolds, and stents; it can also be spun into fibers for sutures.(Abd Alsaheb et al., 2015; Chen et al., 2016; Narayanan, Vernekar, Kuyinu, & Laurencin, 2016; Tyler, Gullotti, Mangraviti, Utsuki, & Brem, 2016) The reason for such a wide array of applications comes from the ability to manipulate its properties by controlling stereochemistry and incorporating copolymers,(Becker, Pounder, & Dove, 2010) adding fillers,(Raquez, Habibi, Murariu, & Dubois, 2013) or tuning processing conditions, all of which can have significant impact on crystallinity.(Anderson, Schreck, & Hillmyer, 2008; Rasal, Janorkar, & Hirt, 2010) However, the longer term impact of processing, especially via FDM, on degradation has not been examined, to the best of our knowledge.

The degradation of PLA is known to proceed in stages that depend on the processing and properties of the PLA. Generally, water diffuses into the PLA part and is consumed by the hydrolytic reaction. The hydrolysis reaction is thought to have a higher rate near the chain end, where a hydroxyl group can promote the reaction. However, chain scission also occurs along the backbone, albeit at a slower rate. The effect of chain ends on degradation rate manifests as a number-averaged molecular weight (M_n) dependence of degradation rate. M_n dependence is only observed below 4×10^4 g/mol.(Gorrasi & Pantani, 2018) Since the degradation reaction rate increases with decreasing pH below 4 and increasing pH above 8,(Gorrasi & Pantani, 2018) the reaction becomes self-catalytic if degradation products cannot diffuse away, i.e. accumulation of lactic acid lowers the pH locally. In later stages, degradation of oligomers by microbes can become important. Due to the complexity of biodegradation, most research has focused on the more readily quantifiable hydrolytic degradation that must precede biodegradation.(Gorrasi & Pantani, 2018).

Temperature is an important parameter in PLA degradation. Due to its interest for biomedical applications, much research has focused on degradation at 37 °C, which is below the glass transition temperature (T_g) of PLA. The other major focus has been the compostability of PLA, which has prompted studies for the most part in the range of 50 to 80 °C. Much of this range is above the T_g of PLA (~60 °C). The activation energy for PLA degradation rate (determined by reduction in PLA M_n) changes at T_g. It is significantly greater below T_g than it is above T_g.

Crystallinity can also play a role in PLA degradation. Processing of PLA has a significant impact on degree of crystallinity, and therefore degradation rate. In the case of injection molding and FDM 3D printing (the focus of this study), rapid cooling in the absence of nucleating agents leads to very low degrees of crystallinity.(Masutani & Kimura, 2018) Of course, the crystal structure and degree of crystallinity are also a function of the stereochemistry of PLA.(Masutani & Kimura, 2018) The majority of research efforts have focused on the impact of stereochemistry of well-defined polymers with narrow molar mass distribution, which has been crucial for establishing the fundamental understanding of PLA behavior. It is now important to extend such understanding to less well-defined PLA that is commercially relevant. Due to the commercial availability of L-lactide (from commercial fermentation), commercial PLA contains 92 to 100% poly(L-lactide) (PLLA). Unlike laboratory PLLA, commercial PLA tends to have a much broader molar mass distribution ($Đ$) as well as agents added to improve processing and performance. A study on solution cast PLA found that, initially, commercial PLA degrades more rapidly than PLA synthesized at laboratory scale.(Höglund, Odelius, & Albertsson, 2012) However, at long times M_n of the two types of PLA decreased at the same rate. Conversely, the physical properties of the laboratory scale PLA declined more rapidly than those of the commercial PLA. Although not proposed by the authors of the original study, both trends can be explained by the fact that the laboratory PLA had narrower $Đ$ than the commercial PLA. Thus, the importance of studying degradation of commercial PLA has recently been recognized.(Gorrasi & Pantani, 2018) One study has examined the impact of FDM processing on degradation of commercial PLA filament by focusing on the importance of print direction.(Gonzalez Ausejo et al., 2018) The main conclusion of the study is that horizontal FDM printing yields initial mechanical properties that are superior to vertical FDM printing, because proximity to the heated build plate results in better interlayer adhesion. A limited

number of mechanical property measurements as a function of degradation time at 0, 3, and 7 days and 50 °C was reported, but no clear trend was found.

The purpose of the present study is to extend studies of PLA degradation, at several temperatures, to commercially available PLA filament for FDM 3D printing. Degradation has been tracked by weight, dimensions, and M_n. Since mechanical properties are one of the most important factors to be considered in 3D-printed parts,(Yao et al., 2019) the primary focus of this study is on the change of elastic storage modulus with degradation time. Measurements have been taken at more frequent intervals than previously reported. The results of this study indicate that it is possible to quantitatively analyze degradation rate from the perspective of mechanical properties, which, to our knowledge, has not been previously reported.

2. Methods

2.1 Materials

Natural clear poly (lactic acid) (PLA, glass transition temperature Tg = 56 °C and melting temperature Tm = 157 °C) was provided by 3D Solutech. Deionized (DI) water (resistivity ≅18.2 MΩ cm) was generated by a Milli-Q water purification system. Ultra-High-Grade tetrahydrofuran (THF, Millipore-Sigma) was used as received.

2.2 Samples

Dogbone structures were 3D printed with a design following a standard method for testing tensile properties of plastics. The sample dimensions followed American Society for Testing and Materials (ASTM) standard D638, Type V, with gauge width of 3.18 mm, gauge length of 7.62 mm, and thickness of 0.29 mm. Printing was conducted with a Monoprice Select Mini V2. The parameters used in printing followed the 2019 Cura 'Ultra Fine' settings with layer height set to 0.044 mm, initial layer height set to 0.088 mm, layer width set to 0.35 mm, nozzle temperature set to 200 °C, bed temperature set to 60 °C, and infill set to 80%. These settings generated a crosshatched structure of 8 layers. After printing, some samples were cut for Dynamic Mechanical Analyzer (DMA) measurements to reduce the length to approximately 15.5 mm.

2.3 Degradation

The samples were placed in 40 mL amber vials containing deionized water which were then submerged in silicone oil baths at 37, 50 and 75 °C. These vials were maintained at these temperatures throughout experiments. Each sample was measured before degradation and during degradation at 1, 9, 21, 45, and 68 hours until the samples yielded under stress or the end of experimentation. At each measurement time, samples were removed from water and dried under vacuum at 37 °C overnight. The samples were then weighed, measured, and returned to their vials for further degradation.

2.4 Weight and Dimensional Measurements

The dimensions of the samples were measured using a Mitutoyo micrometer for the thickness of the dogbone structure with a resolution of 0.001 mm. The width of the samples was measured using a General Ultratech caliper with a resolution of 0.01 mm. The weight of the samples was measured to determine material erosion with an AND GH-202 scale with a resolution of 0.1 mg.

2.5 Size-exclusion Chromatography

Molar mass and polydispersity data were obtained on an Agilent–Wyatt combination triple detection size exclusion chromatography (SEC) instrument containing an Agilent 1260 infinity series pump, degasser, autosampler, and thermostatted column chamber set to a column temperature of 30 °C. The columns used are three sequential Agilent PLgel 5 µm MIXED-C columns of 300 mm length and 7.5 mm inner diameter. The Wyatt triple detection unit hosts a miniDawn TREOS 3-angle light scattering detector, a Viscostar II differential viscometer, and an Optilab TrEX refractive index detector. The RI detector was calibrated with a set of narrow dispersity polystyrene standards with molar masses ranging from 2 kDa – 1800 kDa. The mobile phase used was THF at a flow rate of 1.0 mL/min. Samples were prepared at concentrations of approximately 5 mg/mL in THF and filtered through 0.45 µm PTFE syringe filters before injection. ASTRA 6.1 software was used for data analysis.

2.6 Dynamic Mechanical Analysis

The complex tensile modulus of the samples was measured at each specified time interval with a Dynamic Mechanical Analyzer, DMA 2980, TA Instruments. The samples were attached to the instrument by clamping each end between flat plates. They underwent oscillatory tensile measurements from 1 to 200 Hz with a preload force of 0.1 N and a gauge length of 12 to 17 mm at room temperature. The amplitude of the applied force was 0.1 N, which

translates to approximately 0.1 MPa applied stress amplitude. This resulted in a strain amplitude on the order of 0.01%. Thus, all reported moduli are measured within the linear viscoelastic regime.

2.7 Optical Microscopy

Optical images were captured using an Olympus IX70 Microscope (Olympus, Melville, NY) under bright fields. Images were taken at 100x and 200x magnification for a comprehensive illustration of the scaffolding and interlayering 3D structure of the prints.

3. Theory

3.1 Degradation

When considering the degradation of polymers in biomedical applications, there exists three commonly referred modes of erosion that are depicted schematically in Figure 1. Surface erosion, shown in Figure 1(a), is due to hydrolytic reaction at the surface of polymer, independent of solvent diffusion. Degradation at the surface occurs when solvent cannot penetrate the sample or when solvent sorption is much slower than reaction. This can decrease the sample dimensions and alter the shape of the sample. Bulk erosion, shown in Figure 1(b), is caused by solvent molecule diffusion into the bulk of the polymer and hydrolytic degradation homogeneously. This can sever the links between crystalline regions and/or reduce topological entanglements in amorphous regions. Autocatalytic nucleation erosion, shown in Figure 1(c), occurs when products cannot diffuse away, which impacts pH and accelerates degradation rate locally.

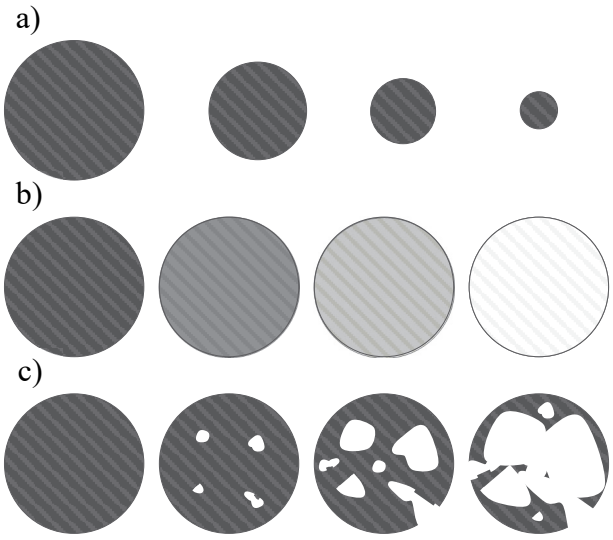

Figure 1. Degradation by a) surface erosion, b) bulk erosion and c) nucleation erosion

These modes are primarily determined by dimensions of the part and degree of crystallinity. Dimensions are important because PLA degradation is a diffusion-reaction problem that requires simultaneous 1) diffusion of water into the polymer, 2) reaction of water with the polymer forming degradation products such as lactic acid, and 3) diffusion of the products out of the polymer. Since the characteristic time for diffusion scales with length squared but reaction is not dependent on length, a scaling argument can be used to show that parts with dimensions of less than 2 mm will undergo bulk erosion,(Gorrasi & Pantani, 2018) while larger dimensions prevent degradation from occurring homogeneously throughout the part. Furthermore, crystals act as impermeable barriers to diffusion and retard the reaction due to inaccessibility of the bulk of the crystal to water. The presence of crystals can have an even greater impact on the diffusion of larger molecular weight products. Localization of the autocatalytic products, lactic acid and water, will result in nucleation erosion. The sample is not limited to only one form of degradation but rather can undergo varying levels of each erosion mode. Due to the dimensions of the samples used in this study, samples are expected to degrade primarily via the bulk erosion mechanism.

The efforts to model degradation of PLA are rather limited. An obvious approach to measure PLA degradation is via mass loss. However, mass loss tends to occur in the final stages of degradation when degradation is so significant that small molecule products are formed that can diffuse away. Another approach is to examine the change in M_n. In one study, a first-order rate law for the degradation reaction was found to reproduce the

experimentally observed exponential decrease of M_n.(Höglund et al., 2012) In another study, a second-order rate law was shown to better capture the behavior of M_n reported in several different literature reports.(Santonja-Blasco, Ribes-Greus, & Alamo, 2012) The approach to modeling mechanical properties, on the other hand, has been more or less empirical. For example, the rupture envelope of polymers often follows the stress-strain curve of the virgin material. The ultimate stress and strain track back the virgin curve as a function of degradation or aging time.(Verdu, 1994) It will be interesting to reveal if a model developed for M_n-based degradation measurements can be applied to modulus-based degradation measurements.

3.2 Storage Modulus

The complex modulus of a sample can be measured nondestructively using small-amplitude oscillatory tests, such as DMA. In this work, tensile DMA tests were conducted by applying an oscillatory force to the sample and deformation, or strain, was measured. According to Bower,(Bower, 2002) the strain of the sample is considered as:

$$\epsilon = \frac{\Delta L}{L_0}$$

where ϵ is strain, ΔL is the change in length, and L_0 is the initial length. Knowing the width (w) and thickness (h) of the sample, which do not change significantly during small-amplitude measurements, the applied force (F) is easily converted to stress, $\sigma = F/wh$. Considering the oscillatory frequency change of strain in response to the applied stress,(Graessley, 2008) each can be considered as:

$\sigma = \sigma_0 exp(i\omega t)$ and $\epsilon = \epsilon_0 exp[i(\omega t - \delta)]$

where ω is frequency, t is time, δ is the phase lag between applied stress and strain, and $i = \sqrt{-1}$. The complex modulus can be defined as:

$$\frac{\sigma}{\epsilon} = E^* = \left(\frac{\sigma_0}{\epsilon_0}\right)\exp(i\delta) = \left(\frac{\sigma_0}{\epsilon_0}\right)(\cos\delta + i\sin\delta) = E' + iE"$$

where the imaginary part, $E"$, is the loss modulus, and the real part, E', is the storage modulus. The storage modulus is a measure of the stiffness of a sample in response to reversible (elastic) deformation.

4. Results

4.1 Optical Microscopy

To better understand the microstructure of the resultant print structure, the samples were observed under a backlit microscope as shown in Figure 2. Observing the resultant geometry at a higher magnification in Figure 2(b) reveals an uneven print commonly found when pushing the lower limits (finer resolution) of a 3D printer. This results in macropores where water can penetrate into the sample via convection. Thus, water sorption into the dogbone samples of this study generated via 3D printing will be much more rapid than would be observed in samples produced via a mold where macropores are not present. Thus, water sorption into the sample is expected to be much faster than the degradation reaction. The ability for water to equilibrate throughout the sample faster than hydrolysis occurs further confirms the expectation that bulk erosion is the dominant mode of degradation in these samples.

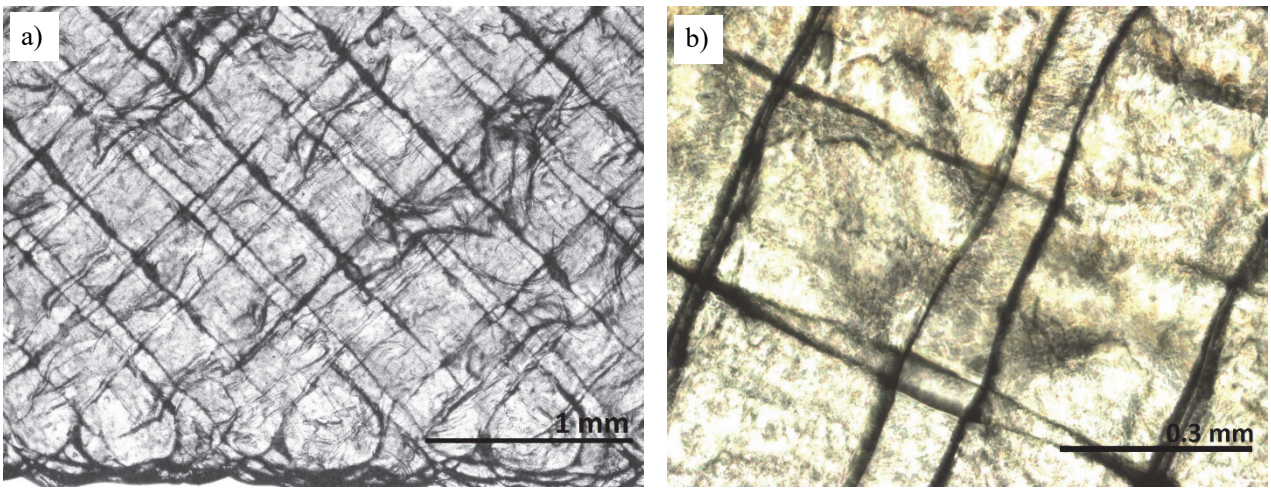

Figure 2. a) A backlit microscopic image of the sample before degradation with a 1 mm scale bar and b) a closer look at the printed structure of the sample before degradation with a 0.3 mm scale bar

4.2 Molecular Weight and Dispersity Changes

Degradation of PLA at 75 °C was monitored by SEC and showed a decrease in M_n from 175 ± 2 kg/mol to 43.2 ± 4 kg/mol after 45 h. However, the dispersity of the PLA sample remained relatively consistent before (1.75 ± 0.05) and after (1.80 ± 0.07) degradation. A reduction in M_n while maintaining consistent chain dispersity is a good indication that degradation was occurring primarily from the ends of the polymer chain, which is consistent with literature observations.(Elsawy, Kim, Park, & Deep, 2017; Gorrasi & Pantani, 2018)

4.3 Weight and Dimensional Changes

All measurements reported in this study are the average and standard deviation of at least three samples. The initial weight and dimensions of each sample set are reported in Table 1. The normalized weight is reported in Figure 3 as a function of degradation time for the degradation temperatures reported in the legend. The reference for normalization is the initial value, such that a normalized value is the fraction of the initial value.

$$\text{Normalized value} = \frac{\text{Measured value}}{\text{Initial value}}$$

The polymer showed no significant weight change at any degradation temperature within the time frame measured. Furthermore, samples at 37 °C were held for an extended period of time and showed no significant change. The inset of Figure 3, shows a closer look for samples held at 50 and 75 °C, which were measured up to 45 hours and also showed no significant change in weight.

Table 1. Initial mass and dimensions of printed PLA sample sets

T (°C)	Initial Mass (mg)	Initial Width (mm)	Initial Thickness (mm)
37	151 ± 3	3.20 ± 0.01	0.290 ± 0.005
50	53 ± 1	3.25 ± 0.07	0.291 ± 0.017
75	51 ± 1	3.28 ± 0.06	0.301 ± 0.009

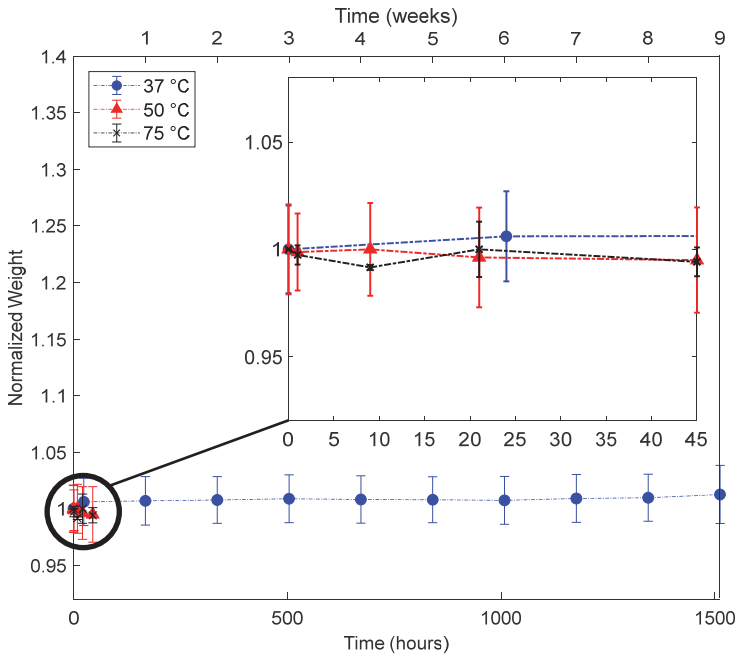

Figure 3. Normalized weight during degradation of PLA samples in deionized water at 37, 50 and 75 °C over 9 weeks. Inset shows the range from 0 to 45 hours. Dashed lines are guides for the eye

The normalized thickness of the samples at 50 and 75 °C in Figure 4(a) showed significant change from initial measurements, increasing with degradation time at early times. Similarly, the normalized width of the samples at 50 and 75 °C in Figure 4(b) showed significant change from initial measurements, decreasing at early degradation times. The change in dimensions is believed to be a result of chain scission which allows chains to rearrange and relax internal stress introduced during the printing process. In other words, shear stresses in the printing nozzle are expected to cause a preferential alignment of polymer chains. This elongation of the end-to-end chain vector is a lower entropy (higher free energy) state than that of a Gaussian coil conformation, which chains adopt in the melt at equilibrium. Chain alignment perpendicular to thickness and net parallel to width results in an increase of thickness and decrease of width upon relaxation of printing stress via chain rearrangement. No significant change was observed in either thickness or width of samples degraded at 37 °C.

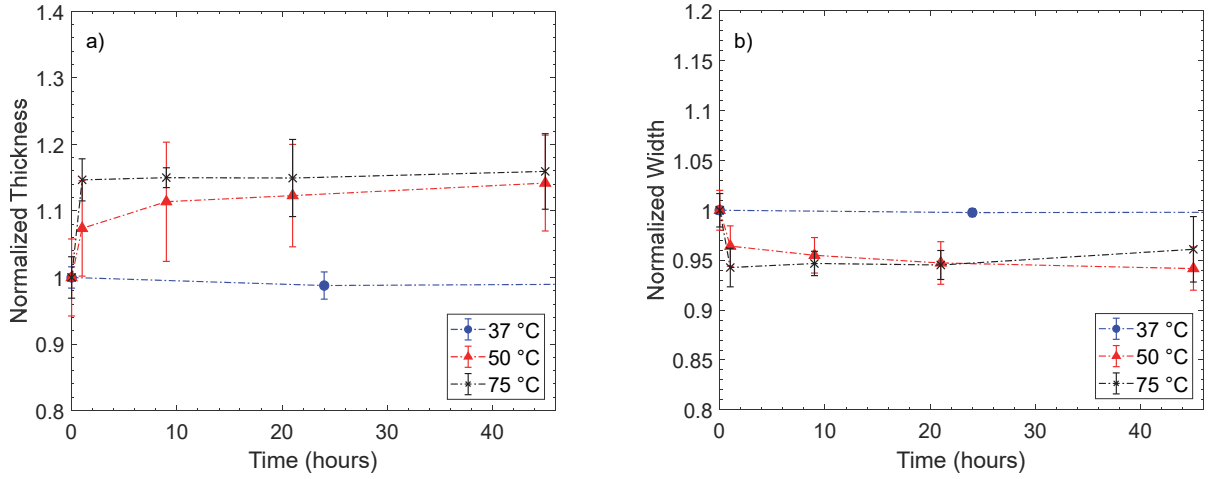

Figure 4. a) Normalized thickness and b) normalized width during degradation of PLA samples in deionized water at 37, 50 and 75 °C. Dashed lines are guides for the eye

4.4 Storage Modulus Change

The storage modulus from the high-frequency plateau is shown in Figure 5(a), and the corresponding loss modulus is shown in Figure 5(b). The storage and loss moduli both follow the same trend with degradation time, indicating an overall change in stiffness of the material without any change of state. In other words, the samples become less stiff but remain solid. The storage modulus changed significantly as a function of degradation time at both 50 and 75 °C, decreasing to a final value about one quarter that of the initial value. Further chain scission beyond the experimental time resulted in the samples being brittle to the point of failure upon handling. Figure 5(a) shows the change of storage modulus during experimentation, which has significant change within one hour. This change in modulus takes the form of an exponential decay and does not follow a second-order rate law. Since the modulus plateaus at a nonzero value, the reaction kinetics models that have been used previously for studies of M_n cannot be used because they predict a decay to zero. Instead, an empirical modeling approach is used. Modeling of the data at 75 °C was not attempted because the rapid modulus decrease resulted in an insufficient number of data points. The following exponential decay equation was regressed to the data at 50 °C using MatLab curve fitting tools:

$$E(t,T) = a\exp(-bt) + c$$

At 50 °C, a is 1112 MPa, b is 1.035 hr^{-1} and c is 482.3 MPa. The decay constant of approximately 1 hour at 50 °C is quite rapid, much faster than M_n changes. These short time measurements have revealed that modulus is an even more sensitive indicator of PLA degradation than M_n.

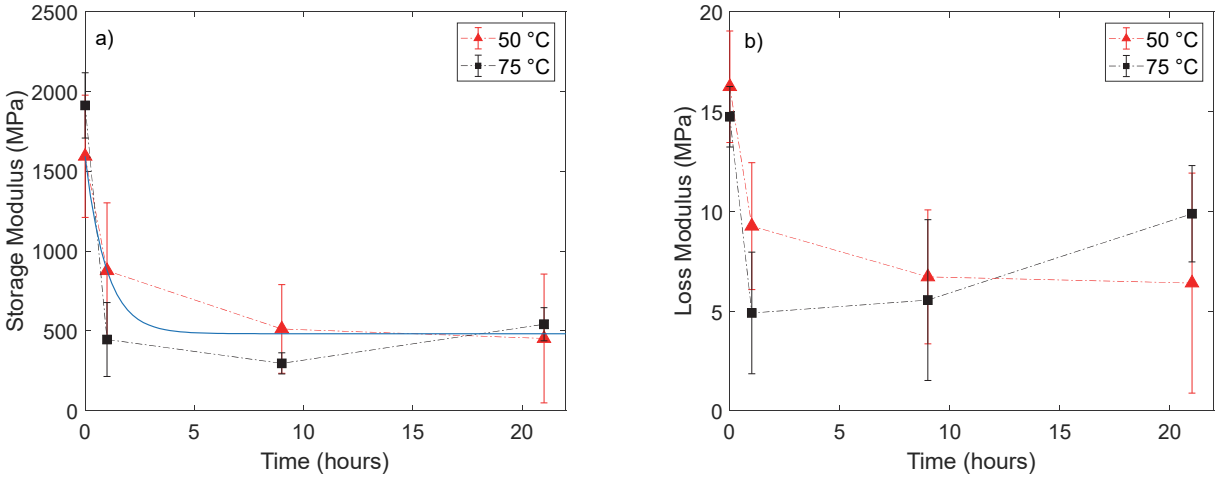

Figure 5. a) Storage modulus and b) loss modulus during degradation of PLA samples in deionized water at 50 and 75 °C. Blue curve is an exponential decay model regressed to 50 °C data. Dashed lines are guides for the eye

5. Conclusions

In this work, degradation of commercial PLA filament for 3D printing was investigated at several temperatures in water. Using optical microscopy, it was found that due to imperfections in line paths porous pathways exist in 3D-printed parts that allow water access to the bulk of the part. This would most likely be the case even for parts much thicker than those used in this study. Although M_n reduced upon degradation, the dispersity remained relatively constant, which indicates that degradation preferentially occurred at chain ends, in agreement with literature.(Elsawy et al., 2017; Gorrasi & Pantani, 2018) Due to the focus on short degradation times, mass loss was not detected over the course of 63 days at 37 °C and 1 to 2 days at 50 and 75 °C. Dimensions also held constant at 37 °C. However, interesting changes in dimensions were observed at early times for samples held at 50 and 75 °C. Specifically sample thickness increased and width decreased over the first day of degradation. Some combination of thermal annealing and chain scission allowed for relaxation of internal stresses/chain alignment that were introduced during the printing process. A rapid decrease in tensile storage modulus with degradation time was detected using DMA. The rate constant for this degradation was 1.035 hr^{-1}, which is much faster than what has been reported for molecular weight decrease due to PLA degradation. This suggests that mechanical properties are the most sensitive measure of PLA degradation. Based on these results and the importance of mechanical strength in many PLA applications, it is important to avoid the exposure of PLA parts to excessively

high temperatures (at least in a wet environment) even for short periods of time. This is particularly true for FDM parts, which have pathways for rapid access of water to the bulk of the part.

Acknowledgments

In fond memory, the authors acknowledge guidance and support provided by Professor Teng Ma. Funding was provided by the CREST Center for Complex Materials Design for Multidimensional Additive Processing (CoManD), NSF award number 1735968. FC acknowledges Research Experience for Undergraduates (REU) support from NSF award numbers 1560337 and 1646897. The authors thank Dr. Rufina Alamo for helpful discussions, as well as Dr. Ayou Hao and the High Performance Materials Institute for training and access to DMA.

References

Abd Alsaheb, R. A., Aladdin, A., Othman, N. Z., Abd Malek, R., Leng, O. M., Aziz, R., & El Enshasy, H. A. (2015). Recent applications of polylactic acid in pharmaceutical and medical industries. *J. Chem. Pharm. Res, 7*, 51-63.

Agrawal, C. M., Huang, D., Schmitz, J. P., & Athanasiou, K. A. (1997). Elevated temperature degradation of a 50:50 copolymer of PLA-PGA. *Tissue Engineering, 3*, 345-352. https://doi.org/10.1089/ten.1997.3.345

Ali Md, H., Batai, S., & Sarbassov, D. (2019). 3D printing: a critical review of current development and future prospects. *Rapid Prototyping Journal, 25*(6), 1108-1126. https://doi.org/10.1108/RPJ-11-2018-0293

Anderson, K. S., Schreck, K. M., & Hillmyer, M. A. (2008). Toughening Polylactide. *Polymer Reviews, 48*(1), 85-108. https://doi.org/10.1080/15583720701834216

Becker, J. M., Pounder, R. J., & Dove, A. P. (2010). Synthesis of Poly(lactide)s with Modified Thermal and Mechanical Properties. *Macromolecular Rapid Communications, 31*(22), 1923-1937. https://doi.org/10.1002/marc.201000088

Bower, D. I. (2002). An Introduction to Polymer Physics. 199-200.

Chen, Y., Geever, L. M., Killion, J. A., Lyons, J. G., Higginbotham, C. L., & Devine, D. M. (2016). Review of Multifarious Applications of Poly (Lactic Acid). *Polymer-Plastics Technology and Engineering, 55*(10), 1057-1075. https://doi.org/10.1080/03602559.2015.1132465

Apparatus and method for creating three-dimensional objects. (1992).

Dorgan, J. R., Lehermeier, H., & Mang, M. (2000). Thermal and Rheological Properties of Commercial-Grade Poly(Lactic Acid)s. *Journal of Polymers and the Environment, 8*(1), 1-9. https://doi.org/10.1023/A:1010185910301

Elsawy, M. A., Kim, K. H., Park, J. W., & Deep, A. (2017). Hydrolytic degradation of polylactic acid (PLA) and its composites. *Renewable and Sustainable Energy Reviews, 79*, 1346-1352. https://doi.org/10.1016/j.rser.2017.05.143

Farah, S., Anderson, D. G., & Langer, R. (2016). Physical and mechanical properties of PLA, and their functions in widespread applications-A comprehensive review ☆ . *Advanced Drug Delivery Reviews*. https://doi.org/10.1016/j.addr.2016.06.012

Gonzalez Ausejo, J., Rydz, J., Musioł, M., Sikorska, W., Janeczek, H., Sobota, M., . . . Kowalczuk, M. (2018). Three-dimensional printing of PLA and PLA/PHA dumbbell-shaped specimens of crisscross and transverse patterns as promising materials in emerging application areas: Prediction study. *Polymer Degradation and Stability, 156*, 100-110. https://doi.org/10.1016/j.polymdegradstab.2018.08.008

Gorrasi, G., & Pantani, R. (2018). Hydrolysis and Biodegradation of Poly(lactic acid). In M. L. Di Lorenzo & R. Androsch (Eds.), *Synthesis, Structure and Properties of Poly(lactic acid)* (pp. 119-151). Cham: Springer International Publishing.

Graessley, W. W. (2008). Chapter 2 Linear Viscoelasticity. In *Polymeric Liquids & Networks: Dynamics and Rheology* (pp. 101-178). New York: Garland Science.

Höglund, A., Odelius, K., & Albertsson, A.-C. (2012). Crucial Differences in the Hydrolytic Degradation between Industrial Polylactide and Laboratory-Scale Poly(L-lactide). *ACS Applied Materials & Interfaces, 4*(5), 2788-2793. https://doi.org/10.1021/am300438k

Jamshidian, M., Tehrany, E. A., Imran, M., Jacquot, M., & Desobry, S. (2010). Poly-Lactic Acid: Production, applications, nanocomposites, and release studies. *Comprehensive Reviews in Food Science and Food*

Safety, 9, 552-571. https://doi.org/10.1111/j.1541-4337.2010.00126.x

Masutani, K., & Kimura, Y. (2018). Present Situation and Future Perspectives of Poly(lactic acid). In M. L. Di Lorenzo & R. Androsch (Eds.), *Synthesis, Structure and Properties of Poly(lactic acid)* (pp. 1-25). Cham: Springer International Publishing.

Mehta, R., Kumar, V., Bhunia, H., & Upadhyay, S. N. (2005). Synthesis of Poly(Lactic Acid): A Review. *Journal of Macromolecular Science, Part C, 45*(4), 325-349. https://doi.org/10.1080/15321790500304148

Narayanan, G., Vernekar, V. N., Kuyinu, E. L., & Laurencin, C. T. (2016). Poly (lactic acid)-based biomaterials for orthopaedic regenerative engineering. *Advanced Drug Delivery Reviews, 107*, 247-276. https://doi.org/10.1016/j.addr.2016.04.015

Raquez, J.-M., Habibi, Y., Murariu, M., & Dubois, P. (2013). Polylactide (PLA)-based nanocomposites. *Progress in Polymer Science, 38*(10), 1504-1542. https://doi.org/10.1016/j.progpolymsci.2013.05.014

Rasal, R. M., Janorkar, A. V., & Hirt, D. E. (2010). Poly(lactic acid) modifications. *Progress in Polymer Science, 35*(3), 338-356. https://doi.org/10.1016/j.progpolymsci.2009.12.003

Santonja-Blasco, L., Ribes-Greus, A., & Alamo, R. G. (2012). Comparative thermal, biological and photodegradation kinetics of polylactide and effect on crystallization rates. *Polymer Degradation and Stability, 98*(3), 771-784. https://doi.org/10.1016/j.polymdegradstab.2012.12.012

Tyler, B., Gullotti, D., Mangraviti, A., Utsuki, T., & Brem, H. (2016). Polylactic acid (PLA) controlled delivery carriers for biomedical applications. *Advanced Drug Delivery Reviews, 107*, 163-175. https://doi.org/10.1016/j.addr.2016.06.018

Verdu, J. (1994). Effect of Aging on the Mechanical Properties of Polymeric Materials. *Journal of Macromolecular Science, Part A, 31*(10), 1383-1398. 10.1080/10601329409350099

Vink, E. T. H., & Davies, S. (2015). Life Cycle Inventory and Impact Assessment Data for 2014 Ingeo™ Polylactide Production. *Industrial Biotechnology, 11*(3), 167-180. https://doi.org/10.1089/ind.2015.0003

Vink, E. T. H., Rábago, K. R., Glassner, D. A., & Gruber, P. R. (2003). Applications of life cycle assessment to NatureWorks™ polylactide (PLA) production. *Polymer Degradation and Stability, 80*(3), 403-419. https://doi.org/10.1016/S0141-3910(02)00372-5

Weir, N. A., Buchanan, F. J., Orr, J. F., Farrar, D. F., & Dickson, G. R. (2004). Degradation of poly-L-lactide. Part 2: Increased temperature accelerated degradation. *Proceedings of the Institution of Mechanical Engineers, Part H: Journal of Engineering in Medicine, 218*, 321-330. https://doi.org/10.1243/0954411041932809

Yao, T., Deng, Z., Zhang, K., & Li, S. (2019). A method to predict the ultimate tensile strength of 3D printing polylactic acid (PLA) materials with different printing orientations. *Composites Part B: Engineering, 163*, 393-402. https://doi.org/10.1016/j.compositesb.2019.01.025

Appendix A

The thermal control set-up is shown in Figure A1 in exploded form. Sample vials were suspended in silicone oil using a custom part (see black part in Figure A1). The temperature of the well-stirred silicone oil was maintained within 0.5 °C of the target temperature using feedback control.

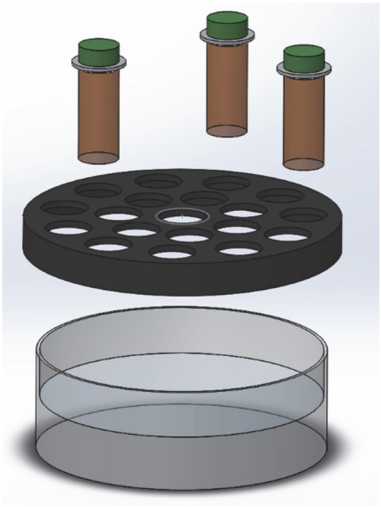

Figure A1. A computer-aided design (CAD) representation of the apparatus used to control temperature during degradation studies of PLA.

Elution curves from the refractive index detector of the SEC are shown in Figure A2 to illustrate the significant change of molecular weight and relatively constant dispersity during degradation. Longer elution time denotes lower molecular weight. Reported M_n and dispersity values come from analysis of Figure A2.

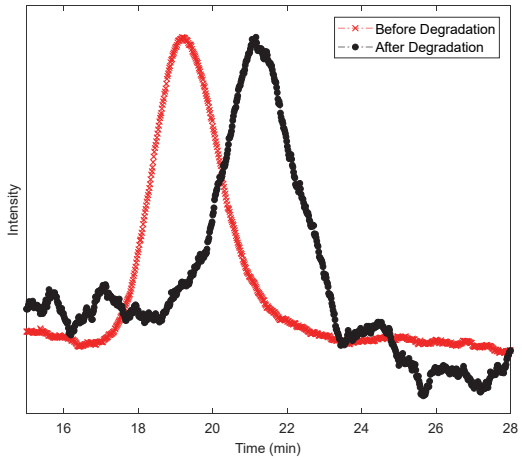

Figure A2. SEC data of normalized refractive index as a function of elution time before (red) and after (black) degradation.